

Conjugated Copolymers Based on Fluorene–Thieno[3,2-*b*]thiophene for Light-Emitting Diodes and Photovoltaic Cells

Wei-hua Tang, Lin Ke, Li-wei Tan, Ting-ting Lin, Thomas Kietzke, and Zhi-Kuan Chen*

Institute of Materials Research and Engineering, 3 Research Link, Singapore 117602, Singapore

Received March 9, 2007; Revised Manuscript Received June 15, 2007

ABSTRACT: Alternating conjugated copolymers comprised of 9,9-dihexylfluorene and unsubstituted/substituted thieno[3,2-*b*]thiophene moieties were synthesized using the Suzuki coupling reaction. The structures of these polymers were characterized, and their thermal, photophysical, electrochemical, and electroluminescent properties were investigated. By β -substitution of thieno[3,2-*b*]thiophene moiety with alkyl chain, the thermal, electrochemical, and electroluminescence properties of the resulted polymers were tuned. The polymers exhibited good thermal stability with decomposition temperature (T_d) in the region of 308–431 °C and their glass transition temperatures (T_g) ranging from 126 to 146 °C. Incorporation of β -alkyl chain onto thieno[3,2-*b*]thiophene of the alternating copolymers led to lowered T_d and T_g and blue-shifted maximum wavelengths in both absorption and emission spectra. The influence of β -alkyl substitution on the conformation of the polymer chains was evaluated by simulating the optimized geometries of three model oligomers using density functional theory. Light-emitting diode devices were fabricated with a configuration of ITO/PEDOT:PSS/polymer/Ca/Ag for all the polymers. A device based on fluorene and unsubstituted thieno[3,2-*b*]thiophene polymer (**P2**) exhibited pure green emission with a maximum brightness of 6000 cd/m² and current efficiency of 2.7 cd/A. More importantly, this device demonstrated very good spectral stability and robust emission, with only 21% decay in luminance after 64 h driving at 1 mA of constant current. In addition, the potential application of the copolymers for photovoltaic solar cells was discussed.

Introduction

Great efforts have been undertaken in the past decades to develop flexible and tunable polymeric light-emitting diodes (PLEDs) from conjugated polymers.^{1–4} In order to realize full color display, various emissive colors have been achieved by the design and manipulation of the conjugated backbone structures such as poly(*p*-phenylenevinylene) (PPV),⁵ poly(*p*-phenylene),⁶ polythiophene (PT),⁷ and polyfluorene (PF).^{8,9} Among the three primary colors, red and green emissions have reached the sufficient efficiencies and lifetime to commercialization level, while the pursuit of blue light-emitting materials with long-term stability and good color purity still remains as a challenge.¹⁰

PF and its derivatives are one of the most widely studied blue-light emitters due to their high photoluminescence quantum efficiency and facile color tunability.⁸ However, these materials suffer from poor spectral stability caused by their tendency to form long-wavelength excimers or ketonic defects in solid states.^{9b,11} The general strategies to suppress the red-shifted and less efficient excimer emission are either introduction of a small amount of low-band gap chromophores and bulky side chains into PF backbones or copolymerization with suitable comonomers.^{12,13} For the copolymer approach, the utilization of thiophene-based comonomer is much attractive because of the versatility in its structure modification and thus great ease in electronic tunability.^{7a,14,15} Moreover, different structural regio-regularities arising from side-chain substitutions in PTs offer additional opportunities for tuning electronic properties by controlling the coupling configurations.¹⁶ There have been a few reports on the synthesis of random copolymers of fluorene and thiophene or bithiophene through the Still coupling¹⁷ and the Suzuki coupling reactions.¹⁸ Shim et al. recently synthesized an alternating copolymer of 9,9-dioctylfluorene with unsubsti-

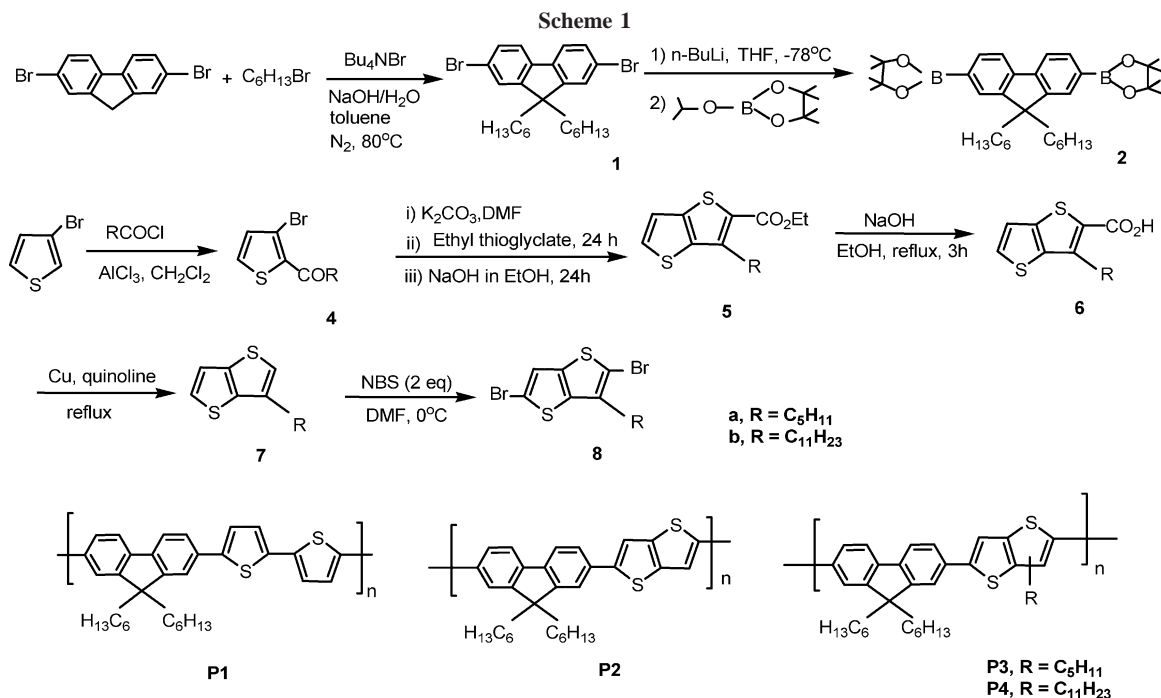
tuted thieno[3,2-*b*]thiophene by Suzuki coupling reactions and investigated its potential applications for PLEDs¹⁹ and field-effect transistors (FET).²⁰ We have also independently investigated the light-emitting and photovoltaic properties of thieno[3,2-*b*]thiophene-based PF copolymers.

In this contribution, we present the synthesis of alternating copolymers of 9,9-dihexylfluorene with bithiophene and unsubstituted or alkyl-substituted thieno[3,2-*b*]thiophene through the Suzuki coupling reaction.²¹ Alkyl substitutions for the thieno[3,2-*b*]thiophene unit and different structural regio-regularities are attained so that we can study the structure–property relationship of the polymers. The general properties of these copolymers, including thermal, optical, and electrochemical properties, are discussed. Furthermore, the potential application of these copolymers as active layers in PLEDs and photovoltaic solar cells is investigated.

Results and Discussion

Synthesis and Characterization. Three new alternating copolymers (**P2–P4**) based on 9,9-dihexylfluorene (FL) and thieno[3,2-*b*]thiophene (TT) were synthesized by using the Suzuki coupling reaction.²¹ The comparable copolymer (**P1**) based on FL and bithiophene was also prepared using the same method. The general synthetic routes and structures of synthesized polymers are shown in Scheme 1. Their chemical structures were verified by ¹H NMR, ¹³C NMR, and MALDI-TOF-MS. The synthesized polymers are all readily soluble in chloroform, THF, and toluene. The number-average molecular weight (M_n) of the synthesized polymers **P1**, as determined by gel permeation chromatography (GPC) using polystyrene as the standards, was 26 300 (PDI, $M_w/M_n = 1.99$). Because of the rigidity of the TT ring, polymers **P2–P4** were found to possess lower M_n , ranging from 8300 to 15 200 with PDI in the 1.8–2.4 region. With increasing the side-chain length of the thieno[3,2-*b*]thiophene unit, the corresponding polymers **P3** and **P4** achieved decreased M_n and larger PDI values due to the steric

* To whom correspondence should be addressed: Fax 65-6872-0785; email zk-chen@imre.a-star.edu.sg.

**Table 1. Molecular Weights^a and Thermal Properties of Polymers**

polymer	yield (%)	M_n	M_w	PDI	DP ^b	T_d^c (°C)	T_g^d (°C)
P1	61	26 300	52 400	1.99	53	436	104
P2	57	15 200	26 800	1.76	32	431	146
P3	46	8 900	21 200	2.38	16	342	126
P4	42	8 300	20 100	2.42	13	308	128

^a Molecular weights determined by GPC using polystyrene standards in THF solutions. ^b Degree of polymerization, with reference to M_n . ^c Decomposition temperature, determined by TGA in nitrogen, based on 5% weight loss. ^d Glass transition temperature, determined by DSC in nitrogen at scan rate of 20 °C/min.

hindrance caused in the coupling reaction. The average repeat unit numbers of the polymers **P1**–**P4** were 53, 32, 16, and 13, respectively. The polymer yields were 42%–61% after purification. These results for the synthesized polymers are summarized in Table 1.

The chemical structures of the synthesized polymers were verified by ¹H NMR and ¹³C NMR spectra. From the ¹H NMR spectra and hydrogen assignment analysis (see in Experimental Section), the signals of fluorenyl, thienyl, and thieno[3,2-*b*]thienyl were clearly observed. For example, **P2**: δ (ppm) 7.55–7.73 (m, 8H, 6 aromatic protons from FL and 2 β -protons from TT unit), 2.05 (br, 4H, protons from 2C₅H₁₁CH₂ of FL), 1.02–1.22 (m, 12H, protons from 2C₂H₅(CH₂)₃CH₂ of FL), 0.77 (m, 10H, protons from 2CH₃CH₂C₄H₈ of FL). The integration indicates that the ratio of FL and TT units in the polymer backbone is 1:1. In the ¹³C NMR spectra of **P1** and **P2**, there are 10 well-resolved signals in the aromatic region and 7 well-resolved signals in the alkyl region for these polymers. For polymer **P3**, the ¹³C NMR spectrum shows 13 well-resolved signals in the aromatic region and 12 well-resolved signals in the alkyl region, indicating the incorporation of β -pentyl group in the TT moiety. It is worthy to note that two kinds of linkage occurred between FL and alkylated TT units when synthesizing regiorandom copolymers **P3** and **P4**. The regiochemistry of these copolymers can be determined by analyzing the α -methylene peaks. When FL and alkylated TT units are in the *cis* configuration, the *cis*- α -methylene peak occurs at ca. 2.77 ppm and the *trans*- α -methylene peak at 2.87 ppm for the *trans*-

linkage between FL and alkylated TT units.²⁸ The relative integration ratios of the *cis*- to *trans*- α -methylene protons of copolymers **P3** and **P4** are 1:1, indicating the equal opportunity of two kinds of linkages when coupling of fluorenyl boronic ester and TT bromo compounds.

Thermal Stability. The thermal stability of the polymers was evaluated by thermogravimetric analysis (TGA), and the results are summarized in Table 1. It is apparent that all the polymers exhibited good thermal stabilities as weight loss less than 5% on heating to 308 °C. Thermal induced phase transition behavior of the polymers was investigated with differential scanning calorimetry (DSC) under a nitrogen atmosphere. The glass transition temperatures (T_g 's) of all polymers are also summarized in Table 1. T_g s of polymers **P2**–**P4** are in the range 126–146 °C. With incorporation of long side chains into the TT unit, polymers **P3** and **P4** generally exhibited lower T_g than nonsubstituted TT-based polymer **P2**. However, all the TT-based copolymers (**P2**–**P4**) showed higher T_g than that of bithiophene-based copolymer **P1** (T_g 104 °C). The increased T_g of **P2**–**P4** should be due to the more rigidity of TT unit than bithiophene structure in the polymer backbone. The relatively high glass transition temperature of conjugated polymers is essential for many applications such as in PLEDs as emissive materials.²²

Optical and Photoluminescence Properties. The spectroscopic properties of all polymers were measured at room temperature in solutions (CHCl₃). The UV–vis absorption and PL spectra of polymers in chloroform (ca. 1×10^{-5} M) are shown in Figure 1 and Figure 2, respectively. Their optical data are summarized in Table 2. Compared with bithiophene-based polymer **P1**, TT-based polymers **P2**–**P4** presented significantly blue-shifted absorption maxima due to the obviously shorter effective conjugation length along polymer backbones. It is noted that **P1** exhibits an absorption λ_{max} at 454 nm, while **P2**, **P3**, and **P4** display shorter λ_{max} at 430, 388, and 383 nm, respectively. Close examination of λ_{max} values for polymers **P2**–**P4** shows a ca. 42 nm red shift in λ_{max} comparing regioregular polymer **P2** to regiorandom polymers **P3** and **P4**. This red shift indicates that regioregular polymer **P2** has a longer effective conjugation length and lower energy π -to- π^* transition compared to those regiorandom polymers. This likely results from

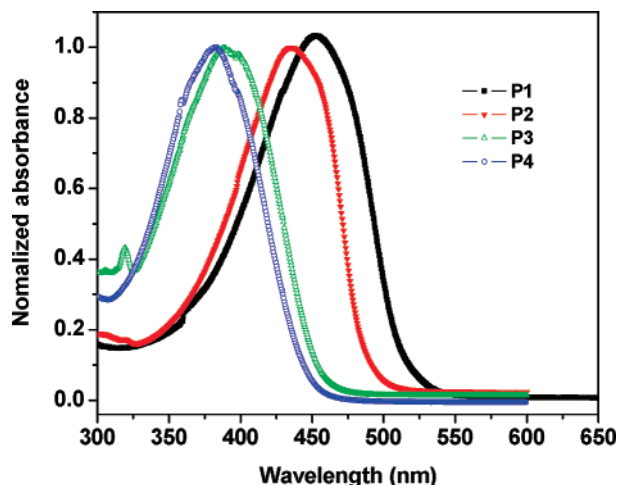


Figure 1. UV-vis absorption spectra of **P1–P4** measured from chloroform solutions ($\sim 1 \times 10^{-5}$ M) at room temperature.

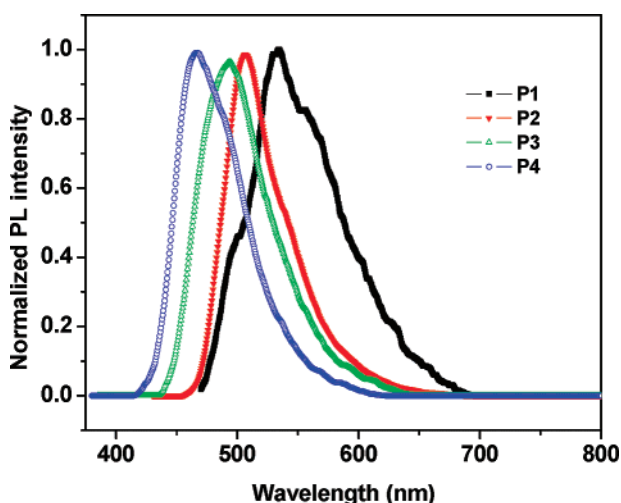


Figure 2. Photoluminescence spectra of **P1–P4** measured from chloroform solutions ($\sim 1 \times 10^{-5}$ M) at room temperature.

the steric repulsion between β -alkyl chain on TT unit and hexyl chains from FL unit, causing a decrease in the effective conjugation length of the polymer chain. Polymers **P3** and **P4** in dilute CHCl_3 solutions display similar λ_{max} (388 and 383 nm, respectively) and onset values: 453 nm (2.74 eV) and 445 nm (2.78 eV), respectively (Figure 1), which indicates the two polymers possess similar effective conjugation length.

Fluorescence spectra of the polymers in CHCl_3 solutions are depicted in Figure 2. The fluorescence spectra of the polymers from **P1** to **P4** were blue-shifted, following the same trend as their absorption spectra, when the polymers were excited at their maximum absorption wavelengths. Polymer **P1** displayed an emission λ_{max} at 534 nm. On contrast, an emission λ_{max} at 508 nm was observed for **P2**. With introduction of a β -alkyl chain

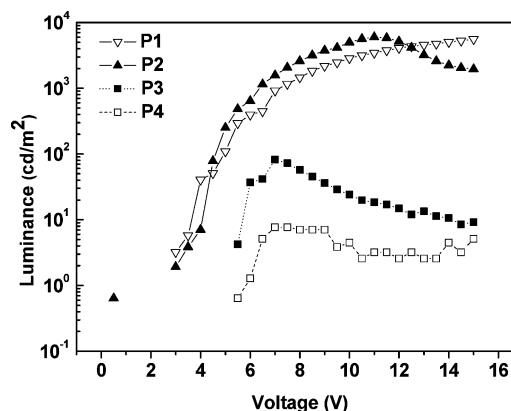


Figure 3. Voltage-luminance (V - L) characteristics of PLEDs from **P1–P4**.

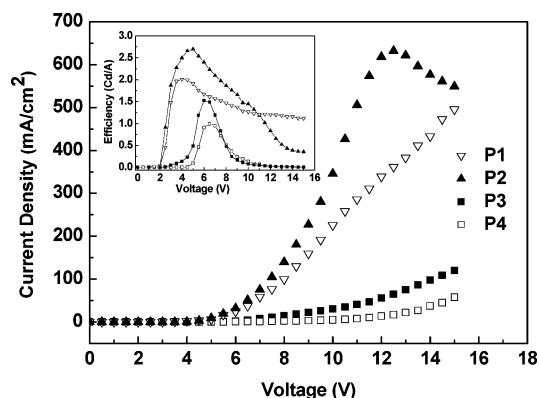


Figure 4. Voltage-current density (V - I) characteristics of PLEDs from **P1–P4**. Inset: voltage-efficiency characteristics of PLEDs from **P1–P4**.

on the TT unit, the emission λ_{max} further shifted to ca. 495 nm for **P3** and 469 nm for **P4** due to the increase of steric hindrance between FL and TT units. The steric hindrance effect of the β -alkyl chain on the optical and electrochemical properties of the polymers will be further elaborated through theoretical calculation.

Electrochemical Property. The electrochemical behavior of the polymers was investigated by cyclic voltammetry (CV). The results of the electrochemical measurements are summarized in Table 2.

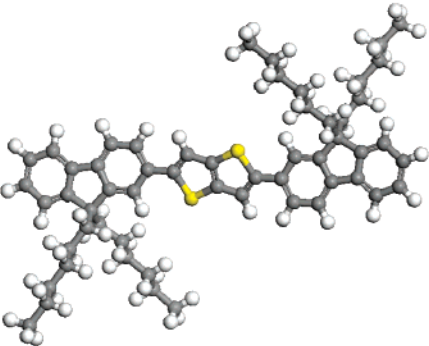
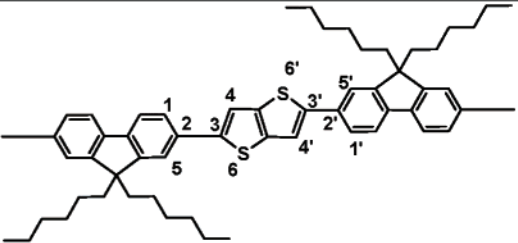
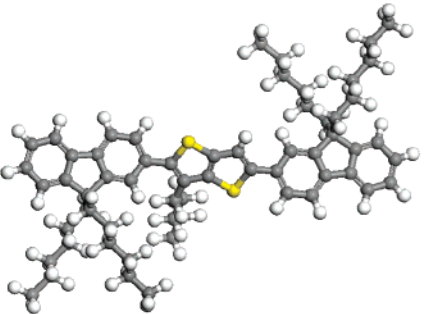
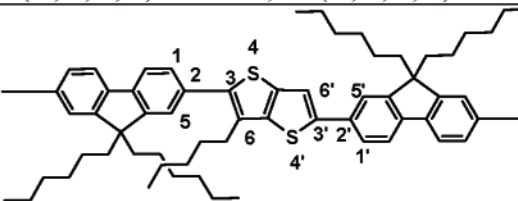
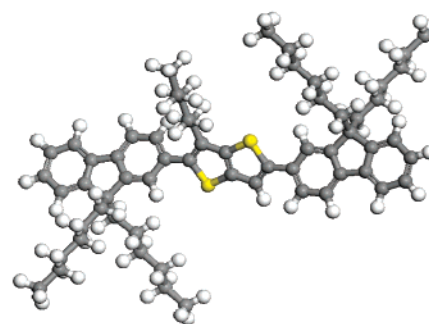
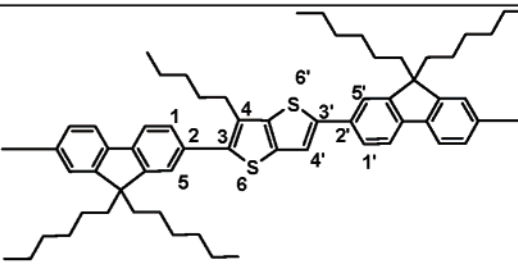
As observed from the cyclic voltammograms, all polymers exhibited partial reversibility in both n-doping and p-doping processes. The onset potentials for oxidation ($E_{\text{ox}}^{\text{onset}}$) were observed in the region of 0.72–0.87 V for polymers **P1–P4**. On the other hand, the onset potentials for reduction ($E_{\text{red}}^{\text{onset}}$) were found in -1.76 to -2.05 V region. From the values of $E_{\text{ox}}^{\text{onset}}$ and $E_{\text{red}}^{\text{onset}}$, the HOMO and LUMO energy levels and band gaps (E_{g}^{ec}) of all polymers were calculated.²³ The HOMO values of polymers **P1–P4** were estimated to be in the range

Table 2. Optical and Electrochemical Properties of Polymers in Chloroform Solutions

polymers	$\lambda_{\text{max}}^{\text{abs}}$ (nm) ^a	λ_{edge} (nm) ^b	$\lambda_{\text{max}}^{\text{em}}$ (nm)	$E_{\text{ox}}^{\text{onset}}$ (V)/ HOMO (eV)	$E_{\text{red}}^{\text{onset}}$ (V)/ LUMO (eV)	optical $E_{\text{g}}^{\text{opt}}$ (eV) ^c	electrochemical E_{g}^{ec} (eV) ^d
P1	454	524	534	0.73/−5.13	−1.76/−2.54	2.36	2.49
P2	430	488	508	0.87/−5.27	−1.82/−2.58	2.54	2.69
P3	388	453	495	0.72/−5.12	−1.98/−2.42	2.74	2.70
P4	383	445	469	0.75/−5.15	−2.05/−2.35	2.78	2.80

^a 1×10^{-5} M in anhydrous chloroform, wavelength of maximum absorbance. ^b λ_{edge} is the onset value of absorption spectrum in long wavelength range. ^c The optical band gap ($E_{\text{g}}^{\text{opt}}$) was obtained from the empirical formula $E_{\text{g}} = 1240/\lambda_{\text{edge}}$ eV. ^d $E_{\text{g}}^{\text{ec}} = E_{\text{ox}}^{\text{onset}} - E_{\text{red}}^{\text{onset}}$ eV, HOMO = $-(E_{\text{ox}}^{\text{onset}} + 4.4)$ eV, LUMO = $-(E_{\text{red}}^{\text{onset}} + 4.4)$ eV.²³

Table 3. Optimized Geometries of Three Model Oligomers (Left Panel) and the Corresponding Dihedral Angles^a

		(a)
		(b)
		(c)

^a The model oligomer structures selected are analogous to the repetition unit for (a) copolymers **P2** and (b) cis and (c) trans Configuration between FL and TT units for copolymer **P3**.

of -5.12 to -5.27 eV, with the LUMO energy levels in the range of -2.35 to -2.58 eV. The band gaps of all polymers were calculated to be in the range of 2.36 – 2.78 eV. Comparing the electrochemistry of regioregular polymers **P1** and **P2** to regiorandom polymers **P3** and **P4**, the regiorandom polymers were found to possess both higher reduction potentials and larger band gaps, indicating that alkylation on TT disrupted the planarity between the FL unit and TT unit of the polymers. This observation is consistent with the measurement of the absorption and emission spectra of the polymers.

The influence of β -alkyl substitution pattern on the optical and electrochemical properties of polymers was appreciated by examining the preferred conformations of models for different linkages. The geometries of three model oligomers (Table 3) were fully optimized using density functional theory (DFT) in the generalized gradient approximation with nonlocal exchange and correlation functions according to Perdew–Wang (GGA-PW91).²⁴ The DFT calculations were performed using the DMol³ module in the Materials Studio Modeling software package (Accelrys Inc.).²⁵ The convergence tolerances for energy change, maximum force, and maximum displacement between optimization cycles were set as 10^{-5} hartree, 0.002 hartree/Å, and 0.005 Å, respectively.²⁶ Self-consistent-field

(SCF) density convergence was 10^{-6} . The orbital cutoff 4 Å was used for all atoms. The dihedral angles were obtained at the final optimized geometries of these model oligomers, with their atomic numbering schemes shown in the corresponding repetition units of copolymers **P2** and **P3**. As shown in Table 3, the average dihedral angles between FL ring and TT ring increased significantly with incorporation of a β -pentyl group in TT ring when comparing the model geometries of model a for **P2** with model b and model c for **P3**. The steric hindrance of the pentyl group resulted in larger dihedral angles at the pentyl-substituted side than unsubstituted side (model c). The cis configuration (model b) brought larger average torsion angles than the trans one (model c). Therefore, a relatively low level of conjugation through the polymer backbone was observed in polymers **P3** and **P4** compared with polymer **P2**, which readily explained the shorter absorption maxima and larger band gaps observed for polymers **P3** and **P4** than **P2**.

Light-Emitting Diode and Photovoltaic Devices. To evaluate the efficiency of three TT-based polymers as emissive materials for light-emitting diodes, PLED devices were fabricated with the configuration of ITO/PEDOT:PSS (20 nm)/polymer (90 nm)/Ca (20 nm)/Ag (200 nm). For simplification, the devices fabricated with polymers **P1**, **P2**, **P3**, and **P4** were

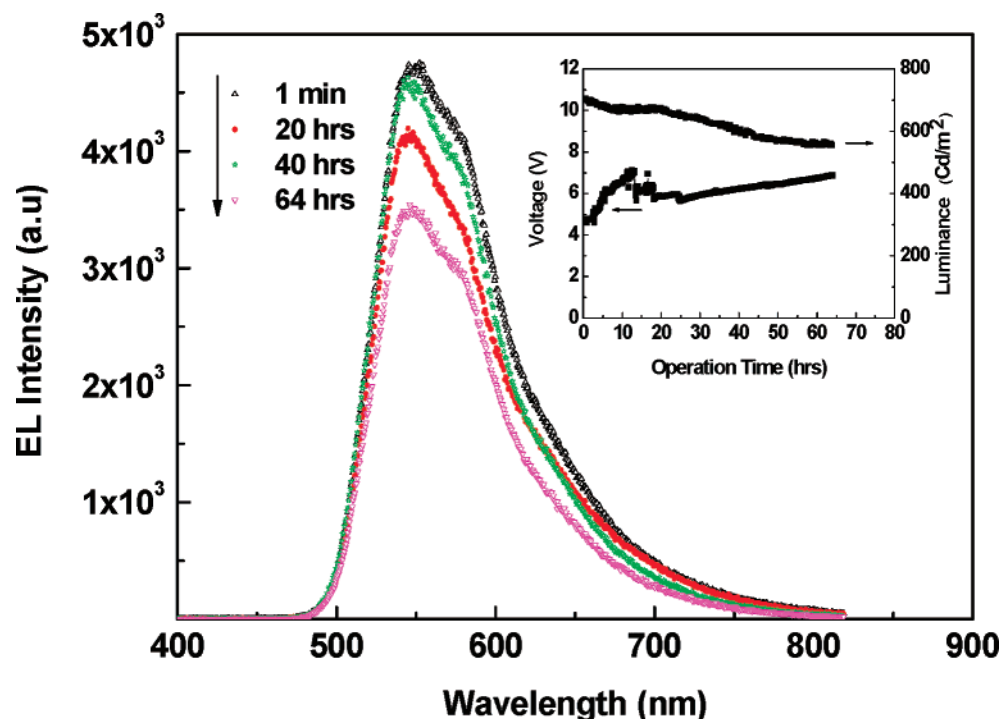


Figure 5. EL spectra of PLEDs from **P2** driven at low noise constant current 1 mA up to 64 h. Inset: voltage and luminance as a function of operation time.

named as device **P1**, device **P2**, device **P3**, and device **P4**, respectively. The voltage–luminescence (V – L) and voltage–current density (V – J) characteristics of the devices are shown in Figure 3 and Figure 4, respectively. The devices **P1** and **P2** showed very low turn-on voltages (V_T). V_T for device **P1** and device **P2** are 2.2 and 2.4 V, respectively, which is lower than the devices based on PFTT and PFT2 with the configuration of ITO/PEDOT:PSS (40 nm)/polymer (80 nm)/LiF (1 nm)/Al (100 nm).¹⁹ The maximum brightness of 6000 and 5560 cd/m² was achieved for devices **P1** and **P2**, which are 6-fold improvement in comparison with PLEDs from PFTT (970 cd/m²) and PFT2 (860 cd/m²).¹⁹ The V_T of devices **P3** and **P4** were 5.2 and 5.8 V with maximum brightness of 82 and 5 cd/m², respectively, which were much poorer than the performance of devices **P1** and **P2**. As depicted in Figure 4, devices **P1** and **P2** exhibit higher current density compared to those of devices **P3** and **P4**. This higher current density may be partially attributed to the morphological effect of polymer films on ITO surface. With regioregular configuration, better structural ordering and alignment of polymer chains was obtained in polymers **P1** and **P2** in comparison to the regiorandom polymers **P3** and **P4**. Loosely and more randomly packed polymer chains in **P3** and **P4** brought thicker injection/transporting barrier for charges and thus lower current density and luminance (Figure 3). The difference in molecular weight of the polymers may also affect the current density in the devices. The average repeat unit numbers in **P1** and **P2** chains are 53 and 32. Their average chain length is much longer than that of **P3** and **P4** (average repeat unit numbers are 16 and 13 for **P3** and **P4**, respectively). Both intrachain and interchain charge transport will be faster in longer polymer chains than in shorter ones. The inset figure of Figure 4 shows the current efficiency vs voltage of the devices for all polymers. It is evident that device **P2** displays the highest current efficiency, nearly double that of devices **P3** and **P4**. The maximum current efficiencies for devices **P1**–**P4** are 2.0, 2.7, 1.5, and 1.0 cd/A, respectively.

The spectral stability of PLEDs remains a challenge for PF-based materials. Figure 5 and Figure 6 show the EL intensity

decay as a function of operation time for devices **P2** and **P1** when driven continuously at a constant current of 1 mA at room temperature. The inset figures depict the voltage and luminance variations with operation time. Clearly shown in Figure 5, device **P2** displays pure green emission with a maximum emission centered at 546 nm. By contrast, device **P1** displays yellow-orange emission with a strong yellow emission at ~580 nm and weaker orange emission at ~615 nm. A ca. 38 and 46 nm bathochromic shift in maximum emission wavelength were observed respectively for **P2** and **P1** in comparison with the corresponding polymers in chloroform solutions. The red shift in maximum emission wavelength was commonly observed for conjugated polymers when transforming from solution to the solid state, mainly due to the better structural ordering and increased planarity of the polymer chains leading to an increased conjugation length.^{27,28} The EL spectra remained stable in both the maximum wavelength and shape even after long-time driving, indicating the suppression of troublesome excimer formation^{9b,11} and thus resulting in stable green emission for device **P2** and yellow-orange emission for device **P1**. As shown in the inset Figure 5, the initial luminance of **P2** is ca. 705 cd/m². After driving up to 64 h, the device displays a luminance of ~525 cd/m², only 21% decay in the initial luminance. The luminance even levels off after being driven 50 h. Actually, the lifetime experiments for devices **P2** and **P1** continued for 1 month and found their robust emission still remained. On the basis of the linear fitting of the curves of luminance against operation time, the lifetimes for devices **P2** and **P1** were estimated to be 1700 and 900 h, respectively. Similar experiments were conducted on devices **P3** and **P4**. Their color stabilities were remained during their shorter lifetime (ca. 10 h). However, two equally strong yellow and orange emissions were observed, and they decayed at the same speed. The poor device efficiency and short lifetime in devices **P3** and **P4** are most likely due to the poor charge transport ability of the polymers in the films, which requires higher electric field to drive the current and then causes the polymer degraded faster.

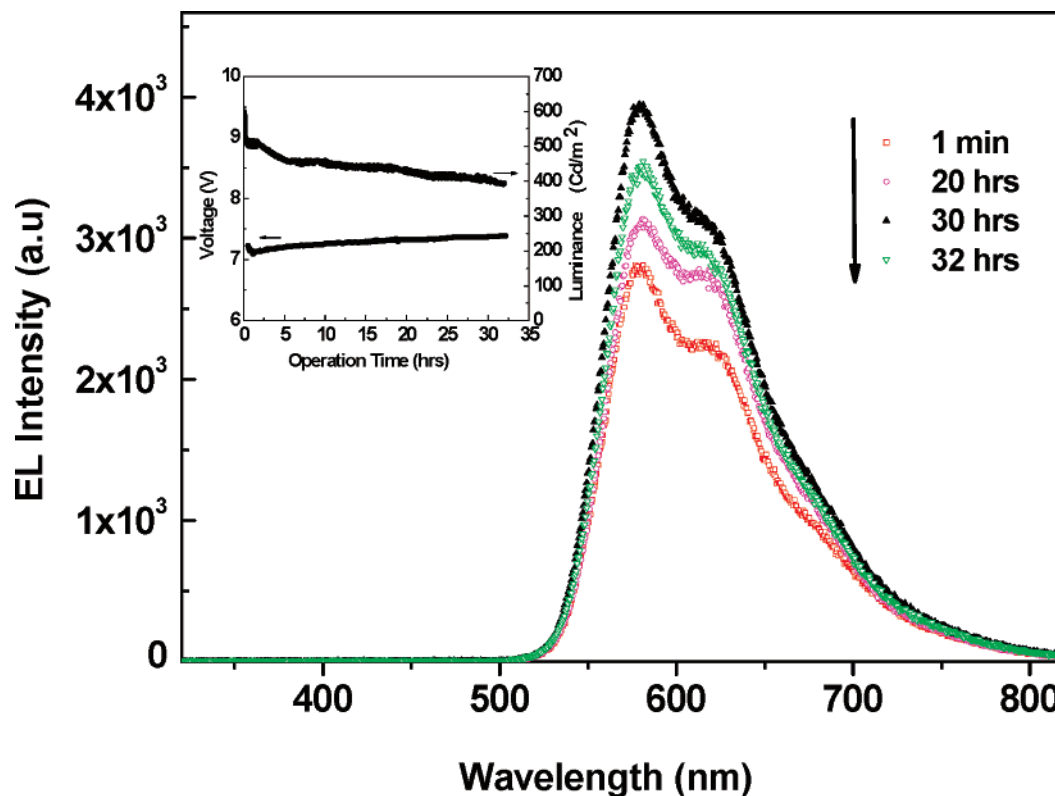


Figure 6. EL spectra of PLEDs from **P1** driven at low noise constant current 1 mA up to 32 h. Inset: voltage and luminance as a function of operation time.

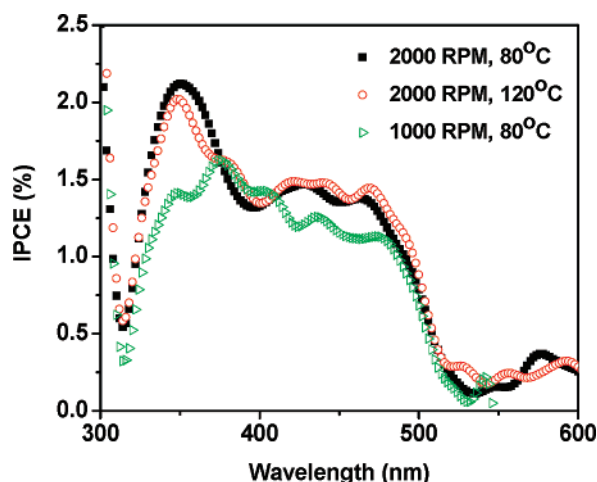


Figure 7. IPCE spectra of the solar cells based on polymer **P2**, prepared at different spin-coating speed and annealing temperature.

Photovoltaic cells with the configuration of ITO/PEDOT-PSS/polymer: PCBM (1:1, w/w)/Ca/Ag were fabricated based on polymers **P2–P4**.²⁹ The incident photon to converted electron current efficiency (IPCE) was found to be extremely low (~2%) leading to limited power conversion efficiencies, partially due to the poor fill factor and narrow range of absorption for the polymers in the solar spectrum. Figure 7 shows the IPCE spectra of polymer **P2**-based solar cells, which were fabricated at different spin-coating speed and annealing temperature. The absorption of all devices only covered the range 300–500 nm.

Conclusions

We have described the synthesis and characterization of new conjugated copolymers comprised of alternating 9,9-dihexy-

lfluorene and substituted or unsubstituted thieno[3,2-*b*]thiophene. Their potential applications in PLED and photovoltaic solar cells are discussed. The polymers were characterized by thermal, optical spectroscopy, cyclic voltammetry, and electroluminescent analysis. Good solubility in common organic solvents and thermal stability, efficient blue-to-green emission, and high glass transition temperatures were demonstrated with these backbone structures. The structure–property relationship was studied with the β -alkylation on the thieno[3,2-*b*]thiophene ring. The optical, thermal, and electrochemical properties of these polymers were very sensitive to the substitution. The PLED device based on poly[2,7-(9,9-dihexylfluorene)-*alt*-thieno[3,2-*b*]thiophene] (**P2**) showed very good device efficiency and excellent emission stability and color purity when being driven at 1 mA of constant current for even 64 h. The application of these polymers in photovoltaic cells is not promising due to low IPCE and narrow absorption in the solar spectrum.

Experimental Section

General Methods. All new compounds were characterized via ¹H NMR and ¹³C NMR spectroscopy using a Bruker 400 MHz DPX FT-NMR spectrometer and mass analysis using a Bruker Autoflex TOF/TOF mass spectrometry. The UV–vis absorption and photoluminescence (PL) spectra were recorded on a Shimadzu UV 3101 spectrophotometer and on a Perkin-Elmer LS-50B luminescence spectrometer, respectively. The number- and weight-average molecular weights of all polymers were determined via GPC on a Waters 2696 instrument, using polystyrene as the standard and THF as the eluent. TGA and DSC were performed under a nitrogen atmosphere at a heating rate of 20 °C/min with DuPont TGA 2050 and TA 2920 analyzers, respectively. The weights of all the samples were in the range 4–6 mg. CV measurements were conducted on a three-electrode AUTOLAB (model PGSTAT30) workstation in a solution of Bu₄NBF₄ (0.10 M) in dichloromethane at a scan rate of 100 mV/s at room temperature under the protection of argon.

Device Fabrication and Characterization. The PLED devices were fabricated with the configuration of ITO/PEDOT:PSS/polymer/Ca/Ag. Commercially available ITO-coated glass substrates were cleaned by sonicating and rinsing in acetone, isopropanol, and deionized water, followed by oxygen plasma treatment. The hole-transporting PEDOT:PSS layer (20 nm) was spin-coated onto ITO, followed by spinning coating the emitting polymer layer (90 nm) from polymer solution in chloroform (7.5 mg/mL). Calcium (20 nm) and silver (200 nm) contacts were deposited sequentially by thermal evaporation through a shadow mask. Thermal evaporation was carried out in a ULVAC system at a base pressure of 2.0×10^{-6} Torr. The resulted devices were protected by encapsulation of a capping glass sealed with epoxy. The current–luminance–voltage (I – L – V) curves were measured using a fully computer-controlled system consisting of a dynamic multimeter (Keithley DMM 2001), a source meter (Keithley 3A 2420), and eight calibrated Si photodiodes. The software was based on LabView. The device lifetime and EL spectrum were performed simultaneously by driving the devices with low noise constant current of 1 mA inside a shielded box.

Synthesis. All starting materials and reagents were purchased from Sigma-Aldrich Chemical Co. and used without further purification. THF was dried over sodium/benzophenone and freshly distilled before use. 2,7-Dibromo-9,9-dihexylfluorene,³⁰ 2,7-bis-(4,4,5,5-tetramethyl-1,3,2-dioxaborolan-2-yl)-9,9-dihexylfluorene,³¹ 2,5-dibromothiopheno[3,2-*b*]thiophene,³² 2,5-dibromo-3-undecylthiopheno[3,2-*b*]thiophene, and 2,5-dibromo-3-pentylthiopheno[3,2-*b*]thiophene²⁸ were prepared accordingly by following the procedure adapted from the literature.

2,7-Dibromo-9,9-dihexylfluorene, 1.³⁰ Yield: 60.2%. ¹H NMR (400 MHz, CDCl₃): δ (ppm) 0.60 (m, 4H), 0.78 (t, J = 7.2 Hz, 6H), 1.04–1.17 (m, 12H), 1.91 (m, 4H), 7.44 (d, J = 1.1 Hz, 2H), 7.46 (d, J = 1.8 Hz, 2H), 7.53 (d, J = 8.0 Hz, 2H). MS (MALDI): m/z = 492.106 (calcd for C₂₅H₃₂Br₂: 492.085).

2,7-Bis(4,4,5,5-tetramethyl-1,3,2-dioxaborolan-2-yl)-9,9-dihexylfluorene, 2.³¹ To a solution of **1** (5.0 g, 10.1 mmol) in THF (100 mL) at -78°C was added 13.3 mL (21.2 mmol) of *n*-butyllithium (1.6 M in hexane) by syringe. The mixture was stirred at -78°C for 30 min. 2-Isopropoxy-4,4,5,5-tetramethyl-1,3,2-dioxaborolane (4.4 g, 23.8 mmol) was added rapidly to the solution, and the resulting mixture was warmed to room temperature and stirred for 24 h. The mixture was poured into water and extracted with ether. The organic extracts were washed with brine and dried over anhydrous MgSO₄. The solvent was removed by rotary evaporation, and the residue was purified by column chromatography (silica gel, 5% ethyl acetate in hexane) to provide 4.1 g (66.2%) product **2** as a white solid. ¹H NMR (400 MHz, CDCl₃): δ (ppm) 0.55 (m, 4H), 0.74 (t, J = 7.2 Hz, 6H), 1.08–0.98 (m, 12H), 1.39 (s, 24H), 2.01 (m, 4H), 7.73 (d, J = 7.2 Hz, 2H), 7.75 (s, 2H), 7.82 (d, J = 7.2 Hz, 2H). MS (MALDI): m/z = 586.511 (calcd for C₃₇H₅₆B₂O₄: 586.437).

2,5-Dibromothiopheno[3,2-*b*]thiophene, 3.³² ¹H NMR (400 MHz, CDCl₃): δ (ppm) 7.17 (s, 2H). MS (MALDI): m/z = 297.982 (calcd for C₆H₂S₂Br₂: 297.794).

1-(3-Bromothiophen-2-yl)dodecan-1-one, 4a.²⁸ To a stirring mixture solution of 3-bromothiophene (17.4 g, 107 mmol) and dodecanoyl chloride (23.4 g, 107 mmol) in CH₂Cl₂ (100 mL), AlCl₃ (13.3 g, 100 mmol) was added in portions over 30 min. The resulting solution was stirred for 3 h at room temperature. Cold water (50 mL) was then slowly added to quench the reaction. The crude product was extracted from the mixture solution with CH₂Cl₂ (3 \times 50 mL). The combined organic layers were washed with brine and dried over anhydrous MgSO₄. Removal of the organic solvent gives the product as colorless liquid mixture (31.6 g, 85.6%) of **4a**. ¹H NMR (400 MHz, CDCl₃): δ (ppm) 0.88 (t, J = 6.8 Hz, 3H), 1.24–1.43 (br, 16H), 1.69–1.77 (tt, J = 7.6 Hz, J = 6.8 Hz, 2H), 3.04 (t, J = 7.6 Hz, 2H), 7.31 (d, J = 5.2 Hz, 1H), 7.60 (d, J = 5.2 Hz, 1H). MS (MALDI): m/z = 346.102 (calcd for C₁₆H₂₅SBrO: 346.078).

3-Undecylthiopheno[3,2-*b*]thiophene-2-carboxylic Acid Ethyl Ester, 5a. To a stirring mixture solution of **4a** (20.7 g, 60 mmol) and

K₂CO₃ (15.5 g, 112.2 mmol) in DMF (150 mL), ethyl thioglycolate (6.97 mL, 63.6 mmol) was added. The resulting mixture solution was stirred for 24 h at ambient temperature. A solution of NaOH (0.64 g, 16 mmol) in ethanol (35 mL) was added, and the reaction was continued for another 24 h. The reaction mixture was poured into water (150 mL) and extracted with ethyl acetate (200 mL). The organic layer was washed with water (4 \times 200 mL) and dried over anhydrous MgSO₄. The crude product of **5a** was obtained by removing organic solvents and used directly for the next step without further purification. ¹H NMR (400 MHz, CDCl₃): δ (ppm) 0.89 (t, J = 6.8 Hz, 3H), 1.24–1.32 (br, 16H), 1.40 (t, J = 7.2 Hz, 3H), 1.69–1.77 (tt, J = 7.6, 6.8 Hz, 2H), 3.16 (t, J = 7.6 Hz, 2H), 4.35 (q, J = 6.8 Hz, 2H), 7.23 (d, J = 5.2 Hz, 1H), 7.51 (d, J = 5.2 Hz, 1H). MS (MALDI): m/z = 366.385 (calcd for C₂₀H₃₀S₂O₂: 366.168).

3-Undecylthiopheno[3,2-*b*]thiophene-2-carboxylic Acid, 6a. To a mixture solution of ester **5a** (48.7 g, 48.7 mmol) in ethanol (160 mL), NaOH (5.4 g, 135.3 mmol) was added. The resulting solution was heated to reflux for ca. 3 h. After starting materials was completely consumed by TLC indication, the solvent was removed in vacuo. 200 mL of water was added to the residue. The pH was adjusted to 1 with 10 M HCl to precipitate the titled product. Recrystallization from hexane gave the product acid **6a** (14.1 g, 82.0%). ¹H NMR (400 MHz, CDCl₃): δ (ppm) 0.88 (t, J = 6.8 Hz, 3H), 1.32–1.46 (br, 16H), 1.72–1.79 (tt, J = 7.6 Hz, J = 6.8 Hz, 2H), 3.19 (t, J = 7.2 Hz, 2H), 7.31 (d, J = 5.2 Hz, 1H), 7.60 (d, J = 5.2 Hz, 1H), 12.9 (br, 1H). MS (MALDI): m/z = 338.264 (calcd for C₁₈H₂₆S₂O₂: 338.137).

3-Undecylthiopheno[3,2-*b*]thiophene, 7a. A mixture of acid **6a** (4.0 g, 11.3 mmol), copper (0.38 g, 5.9 mmol), and quinoline (20 mL) was heated to reflux for 3 h. The resultant solution was concentrated by vacuum distillation. Ethyl acetate (50 mL) was added, and the collected organic layer was washed with 1 M HCl (4 \times 50 mL) and dried over anhydrous MgSO₄. The solvent was removed in vacuo, and the residue was passed through a silica gel column eluting with hexane to yield **7a** (2.2 g, 62.3%). ¹H NMR (400 MHz, CDCl₃): δ (ppm) 0.88 (t, J = 6.8 Hz, 3H), 1.26–1.44 (br, 16H), 1.72–1.80 (tt, J = 7.6 Hz, 6.8 Hz, 2H), 2.73 (t, J = 7.6 Hz, 2H), 6.99 (d, J = 1.2 Hz, 1H), 7.24 (d, J = 5.2 Hz, 1H), 7.35 (dd, J = 5.2 Hz, 1.2 Hz, 1H). ¹³C NMR (100 MHz, CDCl₃): δ (ppm) 14.42, 23.03, 29.01, 29.53, 29.69, 29.75, 29.84, 29.93, 29.99, 30.35, 32.28, 120.26, 122.06, 126.88, 131.04, 135.32, 139.17. MS (MALDI): m/z = 294.428 (calcd for C₁₇H₂₆S₂: 294.147).

2,5-Dibromo-3-undecylthiopheno[3,2-*b*]thiophene, 8a. To a solution of **7a** (0.6 g, 2 mmol) in DMF (15 mL) at 0°C , *N*-bromosuccinimide (0.7 g, 4 mmol) was added in portions over 30 min. After stirring the solution for 3 h at 0°C , water (10 mL) was added, and the mixture solution was extracted with ethyl acetate (3 \times 20 mL). The combined organic layers were dried over anhydrous MgSO₄. After the removal of solvent in vacuo, the residue was subjected to flush column (silica gel) with hexane as eluant. The product was obtained as white solid with a yield of 0.9 g (89.3%). ¹H NMR (400 MHz, CDCl₃): δ (ppm) 0.87 (t, J = 6.8 Hz, 3H), 1.21–1.27 (br, 16H), 1.76–1.82 (tt, J = 7.6 Hz, 6.8 Hz, 2H), 2.67 (t, J = 7.6 Hz, 2H), 7.15 (d, J = 1.2 Hz, 1H). MS (MALDI): m/z = 452.204 (calcd for C₁₇H₂₄S₂Br₂: 451.966).

1-(3-Bromothiophen-2-yl)-hexan-1-one, 4b. ¹H NMR (400 MHz, CDCl₃): δ (ppm) 0.89 (t, J = 6.8 Hz, 3H), 1.28–1.44 (br, 4H), 1.71–1.75 (tt, J = 7.6 Hz, J = 6.8 Hz, 2H), 3.00 (t, J = 7.2 Hz, 2H), 7.08 (d, J = 5.2 Hz, 1H), 7.49 (d, J = 5.2 Hz, 1H). MS (MALDI): m/z = 262.207 (calcd for C₁₀H₁₃SBrO: 261.984).

3-Pentylthiopheno[3,2-*b*]thiophene-2-carboxylic Acid, 6b. ¹H NMR (400 MHz, CDCl₃): δ (ppm) 0.91 (t, J = 6.8 Hz, 3H), 1.32–1.41 (br, 4H), 1.74–1.79 (tt, J = 7.6 Hz, J = 6.8 Hz, 2H), 3.19 (t, J = 7.2 Hz, 2H), 7.29 (d, J = 5.2 Hz, 1H), 7.61 (d, J = 5.2 Hz, 1H), 12.9 (br, 1H). MS (MALDI): m/z = 254.212 (calcd for C₁₂H₁₄S₂O₂: 254.043).

3-Pentylthiopheno[3,2-*b*]thiophene, 7b. ¹H NMR (400 MHz, CDCl₃): δ (ppm) 0.94 (t, J = 6.8 Hz, 3H), 1.35–1.44 (br, 4H), 1.76–1.82 (tt, J = 7.6 Hz, 6.8 Hz, 2H), 2.75 (t, J = 6.4 Hz, 2H), 7.02 (d, J = 1.2 Hz, 1H), 7.27 (d, J = 5.2 Hz, 1H), 7.37 (dd, J =

5.2 Hz, 1.2 Hz 1H). ^{13}C NMR (100 MHz, CDCl_3): δ (ppm) 14.48, 22.85, 28.73, 30.35, 31.97, 120.30, 122.12, 127.25, 135.30, 139.18, 140.43. MS (MALDI): m/z = 210.208 (calcd for $\text{C}_{11}\text{H}_{14}\text{S}_2$: 210.053).

2,5-Dibromo-3-pentylthieno[3,2-*b*]thiophene, 8b. ^1H NMR (400 MHz, CDCl_3): δ (ppm) 0.90 (t, J = 6.8 Hz, 3H), 1.21–1.27 (br, 4H), 1.76–1.82 (tt, J = 7.6 Hz, 6.8 Hz, 2H), 2.68 (t, J = 7.6 Hz, 2H), 7.16 (s, 1H). MS (MALDI): m/z = 368.102 (calcd for $\text{C}_{11}\text{H}_{12}\text{S}_2\text{Br}_2$: 367.872).

Poly[2,7-(9,9-dihexylfluorene)-*alt*-thieno[3,2-*b*]thiophene], P2.²¹ To a three-necked flask was added monomer **2** (0.88 g, 1.5 mmol), 2,5-dibromothieno[3,2-*b*]thiophene (0.45 g, 1.5 mmol), and 3.6 mL of anhydrous toluene. The air-sensitive catalyst $\text{Pd}(\text{PPh}_3)_4$ (2 mol %, 0.034 g) was added into the mixture under a nitrogen atmosphere. Deaerated 2 M aqueous potassium carbonate (2.4 mL, 4.8 mmol) was transferred to the mixture via cannula. The reaction mixture was stirred and heated under nitrogen at 85 °C for 72 h. At the end of polymerization, the terminal boronic ester group was end-capped by adding excess 2-bromofluorene (37.0 mg, 0.15 mmol) and refluxing 12 h. The reaction mixture was cooled to about 50 °C and slowly added to a vigorously stirred mixture of methanol (100 mL) and 1 M aqueous HCl (10 mL). The precipitate was collected by filtration from methanol. The polymers were further purified by Soxhlet extraction in acetone for 2 days to remove oligomers and catalyst residues. The polymer pellets were collected by filtration and precipitation from methanol and acetone. The final product was obtained as a yellow solid with a yield of 0.51 g (58.0%). ^1H NMR (400 MHz, CDCl_3): δ (ppm) 0.77 (m, 10H), 1.02–1.22 (m, 12H), 2.05 (br, 4H), 7.55–7.73 (m, 8H). ^{13}C NMR (100 MHz, CDCl_3): δ (ppm) 14.30, 22.90, 24.24, 30.05, 31.82, 40.79, 55.84, 115.74, 120.35, 120.57, 125.16, 125.34, 134.13, 139.74, 140.87, 146.95, 152.33.

Poly[2,7-(9,9-dihexylfluorene)-*alt*-bithiophene], P1. By following the similar methods, **P1** was synthesized with monomer **2** and 5,5'-dibromo-2,2'-bithiophene. The final product, an orange polymer, was obtained with a yield of 0.47 g (62.8%). ^1H NMR (400 MHz, CDCl_3): δ (ppm) 0.76 (m, 10H), 1.01–1.21 (m, 12H), 2.06 (br, 4H), 7.33–7.72 (m, 10H). ^{13}C NMR (100 MHz, CDCl_3): δ (ppm) 14.29, 22.90, 24.21, 30.05, 31.82, 40.82, 55.78, 120.29, 120.57, 124.11, 124.92, 125.16, 133.43, 137.00, 140.77, 144.30, 152.28.

Poly[2,7-(9,9-dihexylfluorene)-*alt*-2,5-(3-pentylthieno[3,2-*b*]thiophene), P3. By following the similar methods, **P3** was synthesized with monomer **2** (1.1 g, 1.88 mmol) and 2,5-dibromo-3-pentylthieno[3,2-*b*]thiophene (0.72 g, 1.88 mmol). The final product was obtained as yellow solid with a yield of 0.24 g (42.6%). ^1H NMR (400 MHz, CDCl_3): δ (ppm) 0.77 (m, $\text{C}_4\text{H}_9\text{C}_2\text{H}_5$), 0.93 (m, $\text{C}_4\text{H}_9\text{CH}_3$), 1.02–1.25 (m, $\text{CH}_2\text{C}_3\text{H}_6\text{C}_2\text{H}_5$ and $\text{C}_3\text{H}_7\text{CH}_2\text{CH}_3$), 1.74–1.86 (br, $\text{CH}_2\text{C}_2\text{H}_4\text{CH}_3$), 2.05 (br, $\text{CH}_2\text{C}_5\text{H}_{11}$), 2.77 (TT ring- CH_2 , FL-cis-TT), 2.89 (TT ring- CH_2 , FL-trans-TT), 7.46–7.84 (m, aromatic protons from FL and TT). ^{13}C NMR (100 MHz, CDCl_3): δ (ppm) 14.31, 22.91, 24.20, 28.15, 29.55, 30.02, 31.82, 32.14, 40.44, 40.62, 40.81, 55.68, 115.59, 119.50, 119.72, 120.59, 120.97, 124.21, 125.15, 125.32, 129.33, 134.26, 140.82, 146.70, 152.09.

Poly[2,7-(9,9-dihexylfluorene)-*alt*-2,5-(3-undecylthieno[3,2-*b*]thiophene), P4. Brownish-yellow solid (yield, 61.0%). ^1H NMR (400 MHz, CDCl_3): δ_{H} 0.75 (m, $\text{C}_4\text{H}_9\text{C}_2\text{H}_5$), 0.88 (m, $\text{C}_4\text{H}_9\text{CH}_3$), 1.02–1.40 (m, $\text{CH}_2\text{C}_3\text{H}_6\text{C}_2\text{H}_5$ and $\text{C}_3\text{H}_7\text{CH}_2\text{CH}_3$), 1.73–1.84 (br, $\text{CH}_2\text{C}_2\text{H}_4\text{CH}_3$), 2.04 (br, $\text{CH}_2\text{C}_5\text{H}_{11}$), 2.77 (TT ring- CH_2 , FL-cis-TT), 2.87 (TT ring- CH_2 , FL-trans-TT), 7.45–7.80 (m, aromatic protons from FL and TT).

References and Notes

- (1) (a) Friend, R. H.; Gymer, R. W.; Holmes, A. B.; Burroughes, J. H.; Marks, R. N.; Taliani, C.; Bradley, D. D. C.; Dos Santos, D. A.; Brédas, J. L.; Logdlund, M.; Salaneck, W. R. *Nature (London)* **1999**, 397, 121. (b) Rees, I. D.; Robinson, K. L.; Holmes, A. B.; Towns, C. R.; O'Dell, R. *MRS Bull.* **2002**, 27, 451.
- (2) (a) Heeger, A. J. *Solid State Commun.* **1998**, 107, 673. (b) Sheats, J. R.; Antoniadis, H.; Hueschen, M.; Leonard, W.; Miller, J.; Moon, R.; Roitman, D.; Stocking, A. *Science* **1996**, 273, 884.
- (3) Kraft, A.; Grimsdale, A. C.; Holmes, A. B. *Angew. Chem., Int. Ed.* **1998**, 37, 402.
- (4) (a) Hancock, J. M.; Gifford, A. P.; Zhu, Y.; Lou, Y.; Jenekhe, S. A. *Chem. Mater.* **2006**, 18, 4924. (b) Zhu, Y.; Champion, R. D.; Jenekhe, S. A. *Macromolecules* **2006**, 39, 8712.
- (5) (a) Gustafsson, G.; Cao, Y.; Treacy, G. M.; Klavetter, F.; Colaneri, N.; Heeger, A. J. *Nature (London)* **1992**, 357, 477. (b) Greenham, N. C.; Moratti, S. C.; Bradley, D. D. C.; Friend, R. H.; Holmes, A. B. *Nature (London)* **1993**, 365, 628.
- (6) (a) Grem, G.; Leditzky, G.; Ullrich, B.; Leising, G. *Adv. Mater.* **1992**, 4, 36. (b) Tour, J. M. *Adv. Mater.* **1994**, 6, 190.
- (7) (a) Roncali, J. *Chem. Rev.* **1997**, 97, 173. (b) Perepichka, I. F.; Perepichka, D. F.; Meng, H.; Wudl, F. *Adv. Mater.* **2005**, 17, 2281.
- (8) (a) Pei, Q.; Yang, Y. *J. Am. Chem. Soc.* **1996**, 118, 7416. (b) Grell, M.; Bradley, D. D. C.; Inbasekaran, M.; Woo, E. P. *Adv. Mater.* **1997**, 9, 798.
- (9) (a) Kim, J. S.; Friend, R. H.; Cacialli, F. *Appl. Phys. Lett.* **1999**, 74, 3084. (b) Jenekhe, S. A.; Osaheni, J. A. *Science* **1994**, 265, 765.
- (10) Bernius, M. T.; Inbasekaran, M.; O'Brien, J.; Wu, W. S. *Adv. Mater.* **2000**, 12, 1737.
- (11) (a) Scherf, U.; List, E. J. W. *Adv. Mater.* **2002**, 14, 477. (b) Grell, M.; Bradley, D. D. C.; Ungar, G.; Hill, J.; Whitehead, K. S. *Macromolecules* **1999**, 32, 5810.
- (12) (a) Setayesh, S.; Grimsdale, A. C.; Weil, T.; Enkelmann, V.; Müllen, K.; Maghdadi, F.; List, E. J. W.; Leising, G. *J. Am. Chem. Soc.* **2001**, 123, 946. (b) Wong, K.-T.; Chien, Y.-Y.; Chien, R.-T.; Wang, C.-F.; Lin, Y.-T.; Chiang, H.-H.; Hsieh, P.-Y.; Wu, C.-C.; Chou, C.-H.; Su, Y.-O.; Lee, G.-H.; Peng, S.-M. *J. Am. Chem. Soc.* **2002**, 124, 11576.
- (13) (a) Klärmer, G.; Davey, M. H.; Chen, W.-D.; Scott, J. C.; Miller, R. D. *Adv. Mater.* **1998**, 10, 993. (b) Klärmer, G.; Davey, M. H.; Lee, J.-I.; Miller, R. D. *Adv. Mater.* **1999**, 11, 115. (c) Klärmer, G.; Lee, J.-I.; Lee, V. Y.; Chan, E.; Chen, J.-P.; Nelson, A.; Markiewicz, D.; Siemens, R.; Scott, J. C.; Miller, R. D. *Chem. Mater.* **1999**, 11, 1800.
- (14) (a) Andersson, M. R.; Thomas, O.; Mammo, W.; Svensson, M.; Theander, M.; Inganäs, O. *J. Mater. Chem.* **1999**, 9, 1933. (b) Theander, M.; Inganäs, O.; Mammo, W.; Olinga, T.; Svensson, M.; Andersson, M. R. *J. Phys. Chem. B* **1999**, 103, 7771.
- (15) Barbarella, G.; Melucci, M.; Sotigu, G. *Adv. Mater.* **2005**, 17, 1581.
- (16) (a) Faïd, K.; Fréchette, M.; Ranger, M.; Mazerolle, L.; Lévesque, I.; Leclerc, M. *Chem. Mater.* **1995**, 7, 1390. (b) Faïd, K.; Cloutier, R.; Leclerc, M. *Macromolecules* **1993**, 26, 2501. (c) Hou, J.; Tan, Z.; Yan, Y.; He, Y.; Yang, C.; Li, Y. *J. Am. Chem. Soc.* **2006**, 128, 4911.
- (17) Tsuei, B.; Reddinger, J. L.; Scotzing, G. A.; Soloduchko, J.; Katritzky, A. R.; Reynolds, J. R. *J. Mater. Chem.* **1999**, 9, 2189.
- (18) (a) Inbasekaran, M.; Wu, U.; Woo, E. P. U.S. Patent 5777070, 1997. (b) Liu, B.; Yu, W.-L.; Lai, Y.-H.; Huang, W. *Macromolecules* **2000**, 33, 8945.
- (19) Lim, E.; Jung, B.-J.; Shim, H.-K. *Macromolecules* **2003**, 36, 4288.
- (20) Lim, E.; Jung, B.-J.; Lee, J.; Shim, H.-K.; Lee, J.-I.; Yang, Y. S.; Do, L.-M. *Macromolecules* **2005**, 38, 4531.
- (21) Miyaura, N.; Suzuki, A. *Chem. Rev.* **1995**, 95, 2457.
- (22) Tokito, S.; Tanaka, H.; Noda, K.; Okada, A.; Taga, Y. *Appl. Phys. Lett.* **1997**, 70, 1929.
- (23) Chen, Z.-K.; Huang, W.; Wang, L.-H.; Kang, E.-T.; Chen, B. J.; Lee, C. S.; Lee, S. T. *Macromolecules* **2000**, 33, 9015.
- (24) Perdew, J. P.; Wang, Y. *Phys. Rev. B* **1992**, 45, 13244.
- (25) (a) Delley, B. *J. Chem. Phys.* **1990**, 92, 508. (b) B. Delley, *J. Chem. Phys.* **2000**, 113, 7756.
- (26) Lin, T. T.; Zhang, W. D.; Huang, J. C.; He, C. B. *J. Phys. Chem. B* **2005**, 109, 13755.
- (27) Chen, T. A.; Wu, X. M.; Rieke, R. D. *J. Am. Chem. Soc.* **1995**, 117, 233.
- (28) Zhang, X.; Köhler, M.; Matzger, A. *Macromolecules* **2004**, 37, 6306.
- (29) Kiezke, T.; Egbe, D. A. E.; Horhold, H.-H.; Neher, D. *Macromolecules* **2006**, 39, 4018.
- (30) Lee, S. K.; Hwang, D.-H.; Jung, B.-J.; Cho, N. S.; Lee, J.; Lee, D.-J.; Shim, H.-H. *Adv. Funct. Mater.* **2005**, 15, 1647.
- (31) Ranger, M.; Rondeau, D.; Leclerc, M. *Macromolecules* **1997**, 30, 7686.
- (32) Fuller, L. S.; Iddon, B.; Smith, K. A. *J. Chem. Soc., Perkin Trans. 1* **1997**, 3465.

MA070575H